SUPPLEMENTARY MATERIALS

SUPPLEMENTARY VIDEO LEGENDS

Videos show methods at the beginning and then examples of observations that support information provided in the figures and text. All data were repeated at a minimum of 3 times.

Video 1. Reconstructions of non-CF and CF airways showing microdisk movement *in vivo* after methacholine.
Material at the beginning of video shows details related to methods.
Clip A. Large airways reconstructed from CT-based imaging of a non-CF pig. Video is compressed from a real-time duration of 10 min.
Clip B. Large airways reconstructed from CT-based imaging of a CF pig. Video is compressed from a real-time duration of 10 min.

Video 2. Microdisk movement in excised non-CF and CF tracheas submerged in saline.
Material at the beginning of video shows details related to methods.
Clip A. Non-CF. Video is compressed from a real-time duration of 10 min. Microdisks were added to trachea during the 10 min video.
Clip B. CF. Video is compressed from a real-time duration of 10 min. Microdisks were added to trachea during the 10 min video.
Clip C. Microdisks attached to mucus from CF trachea.

Video 3. Mucus strands emerging from submucosal gland ducts and traveling over the surface of non-CF tracheas.
Material at the beginning of video shows details related to methods.
Clip A. Mucus strands labeled with fluorescent nanospheres flow over airway surface. Video is compressed from a real-time duration of 20 min.
Clip B. 3D reconstruction of nanosphere-labeled mucus (green) emerging from submucosal gland duct onto airway surface (grey). Video is compressed from a real-time duration of 10 min.
Clip C. Nanosphere-labeled mucus strand growing from submucosal gland duct, detaching, and traveling over airway surface. Video is compressed from a real-time duration of 7 min.
Clip D. Nanosphere-labeled, anchored mucus stretching and snapping back. Duration = 4 min.
Clip E. Reflected light video of mucus strand growing, detaching, and retracting. Video is compressed from a real-time duration of 3 min.

Video 4. Panoramic videos of static nanosphere-labeled mucus on non-CF and CF tracheas.
Material at the beginning of video shows details related to methods.
Clip A. Non-CF trachea before and after methacholine. Video is compressed from a real-time duration of 1 hr. Methacholine was added at 15 min.
Clip B. CF trachea before and after methacholine. Video is compressed from a real-time duration of 1 hr. Methacholine was added at 15 min.
Clip C. Non-CF trachea in HCO_3^--free saline with bumetanide before and after methacholine. Video is compressed from a real-time duration of 1 hr. Methacholine was added at 15 min.

Clip D. Tethered mucus strands emerging from submucosal gland ducts in methacholine-treated, non-CF trachea bathed in HCO_3^--free saline with bumetanide. Video is compressed from a real-time duration of 12 min.
Clip E. Tantalum microdisks trapped in mucus tethered to submucosal gland ducts in methacholine-treated, non-CF trachea bathed in HCO_3^--free saline with bumetanide. Video is compressed from a real-time duration of 12 min.
Clip F. Tantalum microdisks trapped in mucus tethered to submucosal gland ducts in methacholine-treated, CF trachea. Video is compressed from a real-time duration of 11 min.

SUPPLEMENTARY FIGURE LEGENDS

Fig. S1. Deposition and movement of individual microdisks in the airways of non-CF and CF piglets.
Data are from the 8 CF and 8 non-CF animals shown in Fig. 1. Asterisks indicate $P<0.05$ by ANOVA.
(A) Position of all individual tantalum microdisks after insufflation in all animals relative to the carina (position 0 mm) at the beginning of a tracking run under basal conditions and after methacholine (1.28×10^{-7} mol/kg, I.V.) administration. N=92 microdisks in non-CF piglets under basal conditions, 95 microdisks in non-CF piglets after methacholine administration, 102 microdisks in CF piglets under basal conditions, and 92 microdisks in CF piglets after methacholine administration.
(B) Average position of microdisks relative to carina in each animal at the beginning of tracking run under basal conditions and after methacholine administration.
(C) Maximum speed of all individual microdisks in all animals. See Fig. 1D for average value in each animal in each condition.
(D) Maximum speed of individual microdisks in non-CF and CF piglet.
(E) Mean speed of all individual microdisks in all animals. See Fig. 1E for average value in each animal in each condition.
(F) Percentage of time moving of all individual microdisks in all animals. See Fig. 1F for average value in each animal in each condition.

Fig. S2. Ciliary beat frequency and periciliary liquid depth in non-CF and CF piglets.
(A) Ciliary beat frequency before and after methacholine. N=5 non-CF and 4 CF. * indicates $P<0.05$, paired Student's *t*-test.
(B) Periciliary liquid depth measured 30 min after administering 1.28×10^{-7} mol/kg I.V. methacholine. Left, mean±SEM of 6 non-CF and 4 CF piglets. Right, histogram of all measurements, n= 4,320 non-CF and 2,880 CF.

Fig. S3. Mucus in methacholine-treated non-CF airways.
(A) Scanning electron photomicrograph showing mucus (pseudocolored green) emerging from a submucosal gland after *ex vivo* addition of methacholine (1.28×10^{-5} mol/L). Bar = 10 μm.
(B) Nanospheres (green) colocalize with fluorescently-tagged lectin (WGA) and antibodies to MUC5B and MUC5AC, all in red. Images are stacks of X-Y confocal images of airway surface. Bar = 20 μm. Similar immunostaining and scanning electron photomicrographs were observed in trachea from >3 piglets.

Fig. S4. Methods for preferential visualization of stationary mucus with a large field of view.
Video 4 also provides an illustration of the methodology.
(A) A confocal microscope with a 4x objective collected a series of 32 images in 4 sec. When the 32 images were averaged, stationary mucus was apparent, and moving mucus was not well visualized. Bar = 1 mm.
(B) One image captured a 3.2 mm x 3.2 mm field. To image the entire airway surface, the imaging procedure was repeated to generate a panoramic image by connecting multiple adjacent microscope fields, as shown by the red boxes in a 6 x 5 panoramic image.
(C) Panoramic images were obtained over time. Images in Fig. 4B to 4D are at the end of a 15 min basal period and then 45 min after adding $1.28x10^{-5}$ mol/L methacholine to the bathing solution.

Fig. S5. Globules of mucus at submucosal gland ducts.
(A) Globules of mucus in CF trachea treated with methacholine as in Fig. 4C. Data show 2 examples. The fluorescent nanospheres bound to the surface, but did not penetrate globules, giving the appearance of ring or shell.
(B) Globules of mucus in non-CF trachea treated with methacholine in HCO_3^--free saline containing 10 μm bumetanide as in Fig. 4D. Bars = 0.5 mm.

Fig. S6. Mucus strands fail to detach from submucosal glands when non-CF airways are treated with methacholine in HCO_3^--free saline containing bumetanide.
(A to C). Tracheas were removed from non-CF piglets and images were captured at end of a 15 min basal period and then 45 min after adding $1.28x10^{-5}$ mol/L methacholine. Bar = 1 mm. Data are examples; average data are in Fig. 4F. Tracheas were bathed in **(A)** HCO_3^-/CO_2-free HEPES-buffered (pH 7.4 or 6.8) saline, **(B)** saline containing 10 μM bumetanide, and **(C)** HCO_3^-/CO_2-free saline containing bumetanide. Panel C is the same as shown in Fig. 4D, and is shown here for comparison to panels A and B. The static mucus observed in panel A after methacholine addition was attached to the tracheal edge. Bar = 1 mm. Video 4C.

SUPPLEMENTARY METHODS

Animals

We previously reported generation of *CFTR*$^{-/-}$ pigs (*31*). Here we studied *CFTR*$^{+/+}$ and *CFTR*$^{-/-}$ piglets. Animals were produced by mating *CFTR*$^{+/-}$ male and female pigs. Newborn littermates were obtained from Exemplar Genetics. Animals were studied 8-15 hours after birth. Anesthesia was with ketamine (20 mg/kg, I.M., Phoenix Pharmaceutical, Inc.) and acepromazine (2 mg/kg, I.M., Phoenix Pharmaceutical, Inc.) or xylazine (2 mg/kg, I.M., Lloyd) and sedation was maintained with I.V. propofol (APP Pharmaceuticals). Euthanasia was with I.V. Euthasol (Virbac). The University of Iowa Animal Care and Use Committee approved all animal studies.

In vivo CT-based imaging

To assess mucociliary transport (MCT) *in vivo* in newborn non-CF and CF pigs, we used a previously described X-ray computed tomographic (CT) based assay *(*10). We measured MCT by tracking tantalum microdisks (350 μm diameter x 25 μm thick, Sigma). To deliver microdisks, animals were anesthetized, intubated, and microdisks were insufflated into the airways with a puff of air. Immediately after delivery, the catheter was removed. To avoid the

potential for alterations in the airway surface due to the presence of the delivery catheter, microdisks were not tracked once they traveled above the position of the lung apex. Only microdisks that were delivered beyond the right cranial lobe were tracked to provide enough distance to analyze transport. Thus, the number of tracked microdisks varied between animals and between conditions in an individual animal. The average number (and range) of microdisks shown in Fig. 1 were: non-CF basal = 11.5(4-23), non-CF methacholine = 11.9(2-18), CF basal = 12.8(2-23), and CF methacholine = 11.5(3-19).

CT scans were acquired with a high-resolution multi-row detector computerized tomography scanner (Siemens Somatom, Definition Flash Dual Source 128-slice computed tomography scanner). A series of CT scans were obtained every 15 sec over a 10 min period, and microdisks were tracked over time. Cartesian coordinates (x,y,z) and angular positions in relation to the most anterior portion of the airway were determined visually over time for individual microdisks. Tracking microdisks over time provided multiple instantaneous measurements of microdisk speed. From these speeds, we determined individual microdisk maximum speeds, mean speeds and the fraction of time individual microdisks were in motion. We also quantified animal movement based on anatomical landmarks located at the carina, the opening of the right cranial lobe, and the lung apex. The percentage of time a microdisk was in motion was quantified by dividing the number of instantaneous microdisk speed measurements that were greater than 1 mm/min by the total number of instantaneous microdisk speed measurements x100%. We chose 1 mm/min because this excludes false microdisk movement scoring due to animal movement. In rare cases, animal movement exceeded 1 mm/min. In those circumstances, to avoid falsely scoring a microdisk as moving, microdisks were designated as 'moving' only if microdisk speeds were greater than the calculated animal landmark speeds at the time of instantaneous speed determination.

Microdisk clearance was determined by measuring whether a microdisk left the tracking field or not during the 10 min tracking period. Microdisks that traveled cranial to the lung apex were designated as cleared, and microdisks that remained within the tracking field 10 min after microdisk delivery was designated as not cleared. The percentage of microdisks cleared was determined by dividing the number of cleared microdisks by the total number of microdisks tracked x100%.

To assess *in vivo* mucociliary transport after cholinergic stimulation, we repeated the protocol and measurements in the same animal 5-10 min after administering acetyl-β-methacholine chloride (methacholine, 1.28 $x10^{-7}$ mol/kg, I.V.). We found that larger doses sometimes caused cardiovascular instability during the scanning procedures. This dose is similar to the dose of 1.0 $x10^{-7}$ mol/kg administered I.V. used in a previous CT-based study of 5-7 week old pigs that were paralyzed with pancuronium and mechanically ventilated (*32*). That study found that larger doses sometimes caused hypotension and pneumothorax and noted that the pigs developed pneumothorax with high airway pressures obtained during mechanical ventilation. With 1.28 $x10^{-7}$ mol/kg and higher doses of methacholine, pneumothorax did not occur in our spontaneously breathing newborn piglets. We also used a methacholine dose of $1.28x10^{-7}$ mol/kg for studies in which the trachea was removed and periciliary liquid depth was measured.

Experimental buffers
For most *ex vivo* studies, we used a HCO_3^-/CO_2 buffered Kreb's-Ringer saline containing (in mM): 118.9 NaCl, 25 $NaHCO_3$, 10 dextrose, 2.4 K_2HPO_4, 0.6 KH_2PO_4, 1.2 $CaCl_2$, 1.2 $MgCl_2$, pH 7.35 with 5% CO_2. For some experiments, we used HCO_3^--free HEPES buffered saline containing: 135 NaCl, 5 HEPES, 10 dextrose, 2.4 K_2HPO_4, 0.6 KH_2PO_4, 1.2 $CaCl_2$, 1.2 $MgCl_2$ pH = 6.6 or 7.3). In some preparations, Cl^- transport was inhibited with 10 μM bumetanide, which inhibits NKCC-mediated entry of Cl^- across the basolateral membrane.

Cilia beat frequency
To assess cilia beat frequency (CBF), animals were euthanized and 1 cm long rings of trachea were removed and stored in phosphate buffered saline overnight at 4 °C. The buffer was then changed to HCO_3^-/CO_2 buffered Krebs-Ringers solution at 37 °C for 30 min. A longitudinal cut spanning the length of the tracheal ring was made along the most ventral aspect of the ring to make a rectangular sheet. Tracheal sheets were mounted flat with pins (BioQuip) to dental wax (Electron Microscopy Sciences) and then submerged in 37 °C HCO_3^-/CO_2 buffered Krebs-Ringers solution. We used reflected light to visualize cilia motion (Nikon A1R Resonant Scanning Confocal Microscope, 25x dipping objective at 110 frames/sec). Four independent regions of interest that contained beating cilia were selected at random, and CBF was measured before and after adding 1 μM methacholine. Five videos (interval 2 min, duration 2 sec each) were captured for each condition. A z-axis profile of pixel intensity was generated and used to calculate ciliary beat frequency. Approximately 20 measurements were averaged to generate a CBF value for each animal.

Periciliary liquid depth
Periciliary liquid (PCL) height was measured using methods similar to those we previously reported (*13*) and originally described by Sims and Horne (*33, 34*). Newborn piglets were sedated, received methacholine (1.28 $x10^{-7}$ mol/kg, I.V.), and were euthanized 30 min later. The dose of methacholine was the same as that which we used for the CT-based measurements of MCT *in vivo*. A 1 cm portion of the trachea was immediately removed, immersed in 2% osmium tetroxide dissolved in FC-72 perfluorocarbon (3M), and fixed for 90–120 min. The trachea was then rinsed in FC-72 and dehydrated in three changes of 100% ethanol, one hr each. Both open ends of the tracheas were removed and discarded to avoid areas possibly disturbed during removal from the animal and the samples were trimmed into 2-3 mm wide strips. Tissue near the trachealis muscle was avoided because of variability in liquid height (*33*) and increased folding of the epithelium perhaps due to proximity to contractile muscles. After dehydration, samples were placed in 2:1 100% ethanol:Eponate 12 resin (Ted Pella, Inc.) followed by 1:2 100% ethanol:Eponate 12 for one hr each. Tracheal segments were then infiltrated in 3 changes of 100% Eponate 12 for at least 2 hr each and polymerized for 24 hr at 60 °C. Following processing, four tissue blocks from each trachea were trimmed, thick-sectioned (1 μm) for light-level examination, and stained with Toluidine Blue. Imaging was performed on an Olympus BX-51 equipped with a DP-70 CCD camera (Olympus America Inc.) using a 100×, NA 1.35, PlanApo lens.

PCL height was determined by drawing a line perpendicular to the apical membrane of the epithelial cell surface and ImageJ (NIH) was used for the measurements. Five random images were taken from each of the 4 tissue blocks. On each image, PCL height measurements were

performed at 12 random locations. Three observers who were blinded to the *CFTR* genotype made independent measurements on every image. Thus, the number of measurements per trachea was: 4 tracheal blocks/animal × 5 images/block × 12 measurements/image for 240 measurements per trachea for each observer. Measurements of mucus overlying the PCL were not made, because the mucus often was dislodged during sample preparation. During processing, shrinkage may have occurred, and thus height measurements may underestimate *in vivo* height.

***Ex vivo* assay of tantalum microdisk movement on the tracheal surface**

To assess MCT *ex vivo*, we sedated newborn pigs, administered methacholine ($1.28x10^{-5}$ mol/kg, I.V.) and 30 min later euthanized the animals. For these *ex vivo* studies, we wished to generate copious submucosal gland mucus secretion, and in previous studies, we found that $1.28x10^{-5}$ mol/kg methacholine stimulated abundant secretion of mucus (*28, 35*). It also roughly corresponded to doses of methacholine $1.0x10^{-5}$ mol/L used in other *ex vivo* studies (*16*). Tracheal segments were immediately removed after euthanasia and a longitudinal cut was made along the ventral tracheal surface. Tracheas were mounted flat with pins on dental wax, and the trachea was flooded with 37 °C HCO_3^-/CO_2 buffered Krebs-Ringer solution (pH = 7.35). The volume of saline was 40 ml and extended 500 μm above the airway surface; thus, volume was more than 100-fold greater than periciliary liquid volume.

Over the course of 10 min, microdisks were added to the preparation and rapidly sank to the apical surface. The average number (and range) of microdisks applied to non-CF tracheas were 31(12-47) and to CF tracheas were 26(20-33). Microdisk transport was visualized *en face*. Sequential images were acquired with a camera and a stop-motion video was generated (~0.5 FPS, iPhone, Apple, and Apple iOS Frameography application, Studio Neat). Video was converted to a single channel (Nikon Imaging Systems elements software, Nikon), and channel colors were inverted to produce regions of high intensity at microdisk locations. The positions of microdisks were readily identified with automated tracking software (Imaris, version 7.6.4, Bitplane). A tracking region away from tissue edges and mounting pins was demarcated, automated instantaneous microdisk speed measurements were generated, and the percentage of time microdisks were in motion was determined as the number of instantaneous speed measurements >1 mm/min divided by the total number of instantaneous speed measurements for a given microdisk x100%. See Video 2.

Imaging mucus with fluorescent nanospheres in *ex vivo* tracheal preparations

Tracheas were removed from newborn pigs that were euthanized 30 min after administration of methacholine ($1.28x10^{-5}$ mol/kg, I.V.); as described above, we used this dose to stimulate copious submucosal gland mucus secretion. Tracheal segments ~1 cm long between the opening of the right cranial lobe and the larynx were cut with a surgical blade between cartilage rings and removed from piglets. Tracheal segments were immediately placed in phosphate buffered saline or in the Kreb's-Ringer saline and stored at 4 °C for 1-12 hr. Prior to microscopy, tracheas were transferred to a HCO_3^-/CO_2-buffered Krebs-Ringer solution (pH = 7.35) at 37 °C for 30 min. After 30 min, the tracheas were opened with a longitudinal cut on the ventral aspect and pinned down to a dish containing dental wax. Yellow-green or red fluorescent carboxylate-modified nanospheres (40 nm diameter, FluoSpheres, Molecular Probes) were added and sonicated in saline at a final dilution of 1:20,000. In a few experiments we used sulfate-modified

FluoSpheres and obtained similar mucus labeling. Tracheas were covered with the ~40 ml of nanosphere-containing solution and a depth of ~500 μm over the trachea surface. In a few preparations, tracheas were exposed to experimental buffer that did not contain nanospheres and then nanospheres were added after the formation of mucus strands to test that the nanospheres did not produce the mucus strands. In addition, when we replaced the nanosphere-containing solution with solution that did not contain nanospheres, fluorescence intensity appeared to diminish with time.

Fluorescent nanospheres were visualized using 4x dry, 10x dry, or 25x water-immersion objectives on an upright Nikon A1R resonant scanning confocal microscope. In some preparations, the trachea morphology was simultaneously visualized with reflected light. Experiments were conducted in a temperature-controlled environment (32-35°C). Images and videos showing strand growth, detachment and elasticity were generated with a 10x objective and video confocal microscopy (1 fps). Tantalum microdisks were added to some preparations and were clearly identifiable with reflected light. Reconstructions of strands emerging from submucosal gland ducts were generated from time-lapse of z-series confocal images acquired with a 25x objective. Reconstructions were processed as surface renderings of reflected light and green nanosphere fluorescence (Imaris, version 7.6.4, Bitplane). See Video 3.

Time-averaged panoramic imaging of stationary mucus

To increase the field of view, we created panoramic images, stitching together multiple 4x objective fields (each 4x field = 3.2 mm x 3.2 mm). A confocal microscope was synchronized to a stage controller (MS-2000-500, Applied Scientific Instrumentation, Eugene, OR) that moved the microscope stage to different positions on tracheal preparations. This allowed the generation of panoramic images that encompassed the entire tracheal area. The number of fields required to visualize the entire tracheal surface was dependent on the size of trachea studied; the smallest panoramic image was 4 fields x 4 fields, and the largest panoramic image was 7 fields x 5 fields. Panoramic images typically took 1-2 minutes to acquire, with the time period dependent on the number of individual fields required for a panoramic image. See Video 4.

A single image from a 4x microscopic field does not allow a distinction between moving and stationary mucus. To preferentially image stationary mucus, we applied a time-averaging technique. At each microscopic field, a series of 32 images were acquired over the course of 4 sec. The average pixel fluorescence was computed for the 32 images and a single time-averaged microscopic field was generated. With this time-averaging technique, the signal from stationary fluorescent entities was similar to that in a single image. However, the signal of fluorescent entities in motion was markedly diminished in the time-averaged microscopic field. This time-averaging technique combined with panoramic image acquisition allowed preferential visualization of stationary fluorescent entities on entire tracheal segments. Multiple panoramic images were recorded during a 15 min imaging period, methacholine ($1.28x10^{-5}$ mol/L) was added to the submerged preparations, and panoramic images were acquired for an additional 45 min imaging period.

At the end of the two imaging periods, we counted the number of readily discernable mucus strands and globules that were tethered to the airway surface. Coupling fluorescence and reflected light imaging revealed that adherent mucus exclusively localized with submucosal

gland ducts. In several examples, adherent mucus coverage was so marked that fluorescent strands emanating from dorsally and distally located submucosal gland ducts likely obscured strands emerging from more proximally and ventrally located fields. However, in those examples it was still possible to quantify a large number of distinct adherent entities that localized with structures that were identified as ducts with reflected light. To overcome this limitation, we created a scoring index in which the number of adherent entities on a trachea is represented on a scale of 0-3 with "0" representing 0-5 adherent entities, "1" representing 6-15 adherent entities, "2" representing 15-50 adherent entities, and "3" representing 50 or more adherent entities. Mucus attached to mounting pins and cut tissue edges was clearly distinguishable and was not scored as tethered mucus.

Scanning electron microscopy

Trachea samples were processed for scanning electron microscopy (SEM) using standard procedures. Tissues were fixed overnight with 2.5% gluteraldehyde in 0.1 M cacodylate buffer, post-fixed in 1% osmium tetroxide and dehydrated in a graded series of ethanol washes. Samples were then transitioned to hexamethyldisilizane and air-dried overnight. Tissues were mounted on aluminum stubs, sputter coated with 80:20 gold:palladium and imaged in a Hitachi S-4800 FE-SEM (Hitachi High Technologies America, Inc.)

Fluorescence labeling of mucin

Tracheas that had been treated with methacholine ($1.28x10^{-5}$ mol/L) and exposed to fluorescent nanospheres were fixed by slowly adding an equal volume of 4% paraformaldehyde into the tracheal buffer for a final concentration of 2% paraformaldehyde. Tracheas were fixed for 3 hr at room temperature, permeabilized in 0.03% TX-100 for 30 min at room temperature, and blocked for an additional 2 hr in Super Block (Thermo-Fisher) with 10% normal goat serum (Jackson Immunoresearch). MUC5B and MUC5AC are the two main secreted gel-forming mucins in porcine submucosal glands (*36*). Tracheas were incubated overnight at 4 ˚C in either anti-MUC5B (1:2500, Santa Cruz, clone H-300) or anti-MUC5AC (1:5000, Lab Vision, clone 45M1, ThermoFischer Scientific) antibody. Tracheas were then incubated in Alexa anti-rabbit- or anti-mouse-647 (1:500, Life Technologies, Carlsbad, CA) secondary antibody, respectively. One portion of the trachea was incubated with WGA-rhodamine-594 (1:1000, Invitrogen) without prior permeabilization or blocking. Mucosa and cartilage were separated, the mucosa was placed on slides with DAPI and imaged on an Olympus FV1000 confocal microscope (Olympus) using sequential scanning for each channel.

Statistical analysis

For analyses that compared two groups, we used a paired or unpaired Students *t*-test. For multiple comparisons, we used a one-way ANOVA and Bonferroni post-hoc test. We considered $P<0.05$ statistically significant.

Figure S1

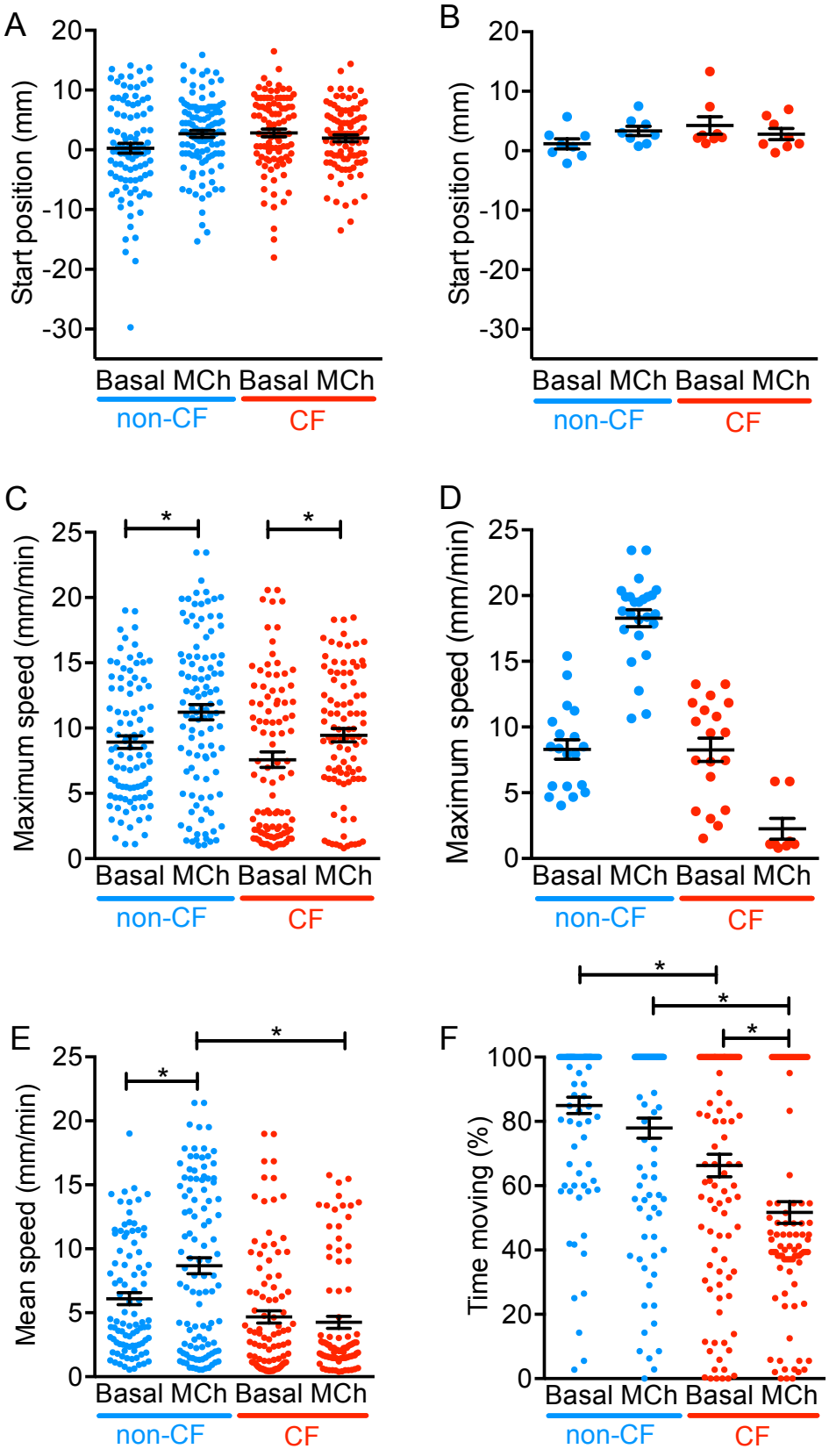
A
Start position (mm)
20
10
0
-10
-20
-30
Basal MCh Basal MCh
non-CF
CF
B
Start position (mm)
20
10
0
-10
-20
-30
Basal MCh Basal MCh
non-CF
CF
C
Maximum speed (mm/min)
25
20
15
10
5
0
*
*
Basal MCh Basal MCh
non-CF
CF
D
Maximum speed (mm/min)
25
20
15
10
5
0
Basal MCh Basal MCh
non-CF
CF
E
Mean speed (mm/min)
25
20
15
10
5
0
*
*
Basal MCh Basal MCh
non-CF
CF
F
Time moving (%)
100
80
60
40
20
0
*
*
*
Basal MCh Basal MCh
non-CF
CF

Figure S2

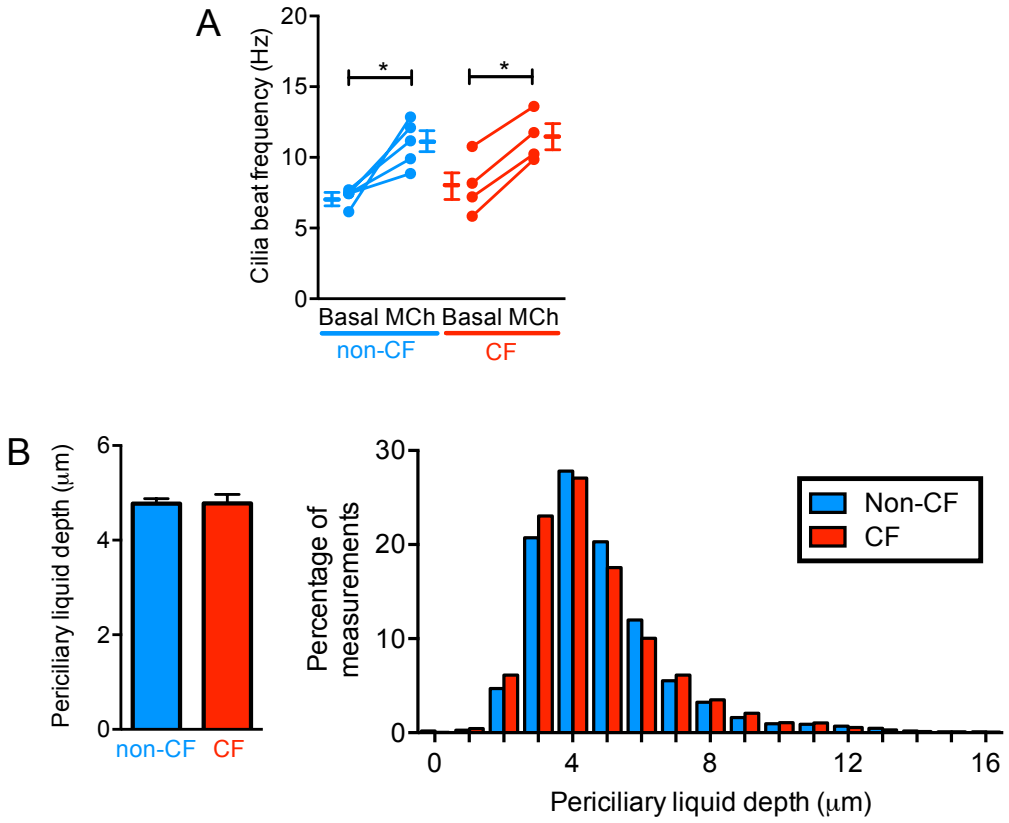
A
Cilia beat frequency (Hz)
20
15
10
5
0
*
*
Basal MCh
Basal MCh
non-CF
CF
B
Periciliary liquid depth (μm)
6
4
2
0
non-CF
CF
Percentage of measurements
30
20
10
0
Non-CF
CF
0
4
8
12
16
Periciliary liquid depth (μm)

Figure S3

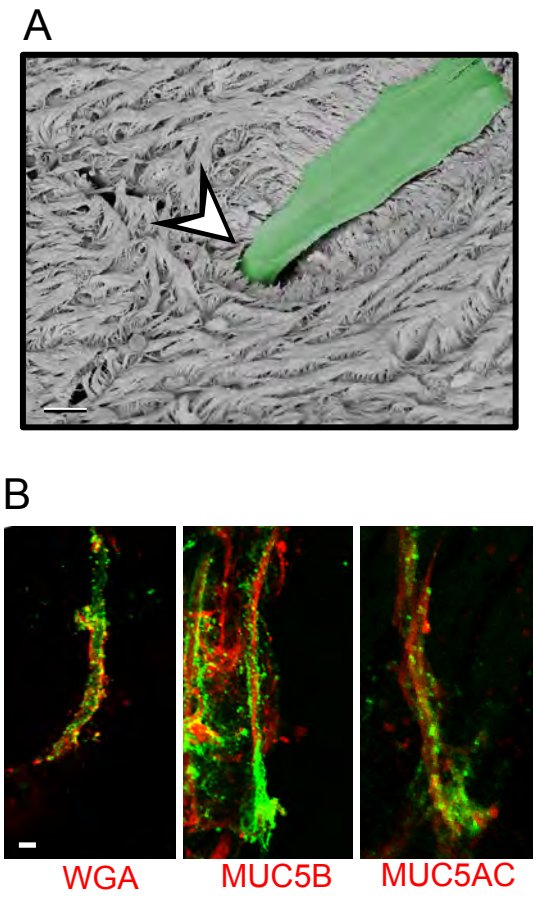

Figure S4

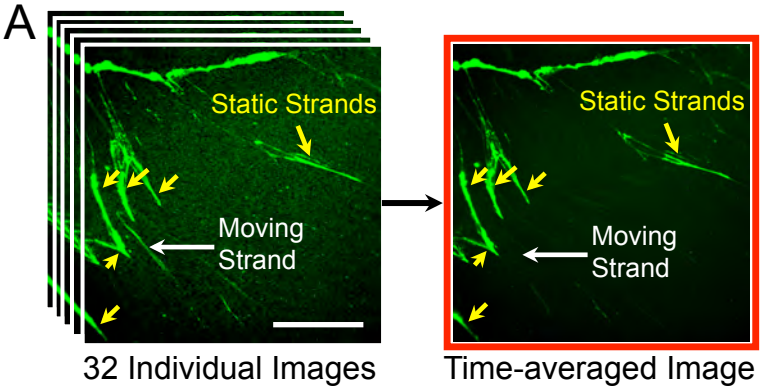
A
Static Strands
Moving Strand
Static Strands
Moving Strand
32 Individual Images
Time-averaged Image

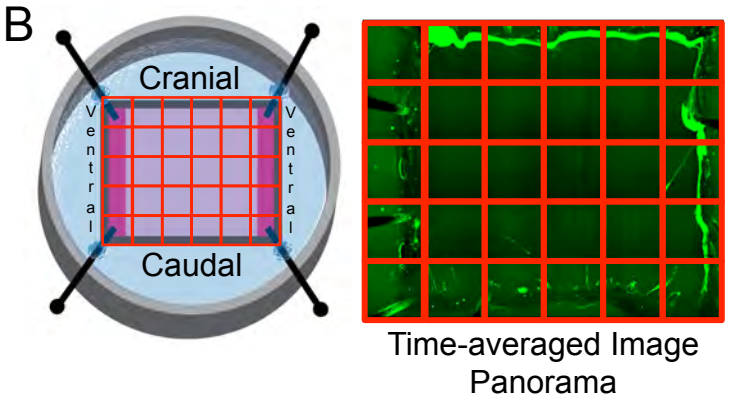
B
Cranial
Ventral
Ventral
Caudal
Time-averaged Image Panorama

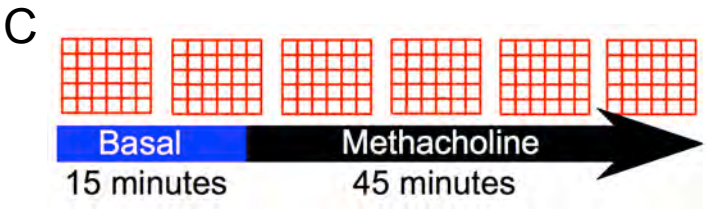
C
Basal
15 minutes
Methacholine
45 minutes

Figure S5

A. CF treated with methacholine

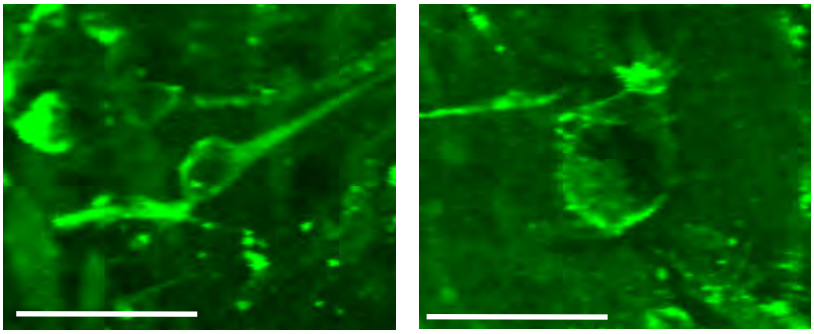

B. non-CF treated with methacholine in HCO_3^--free saline with bumetanide

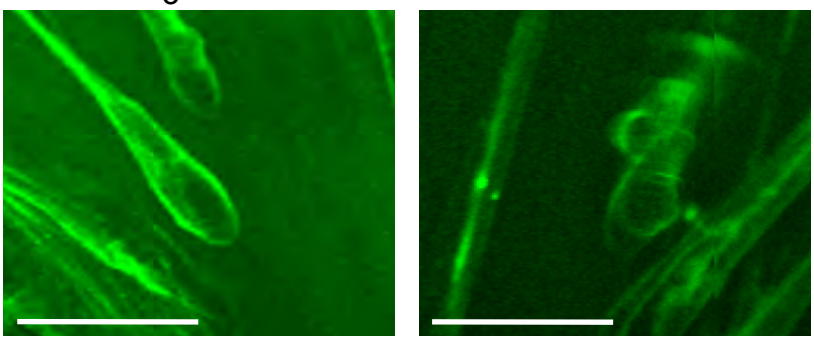

Figure S6

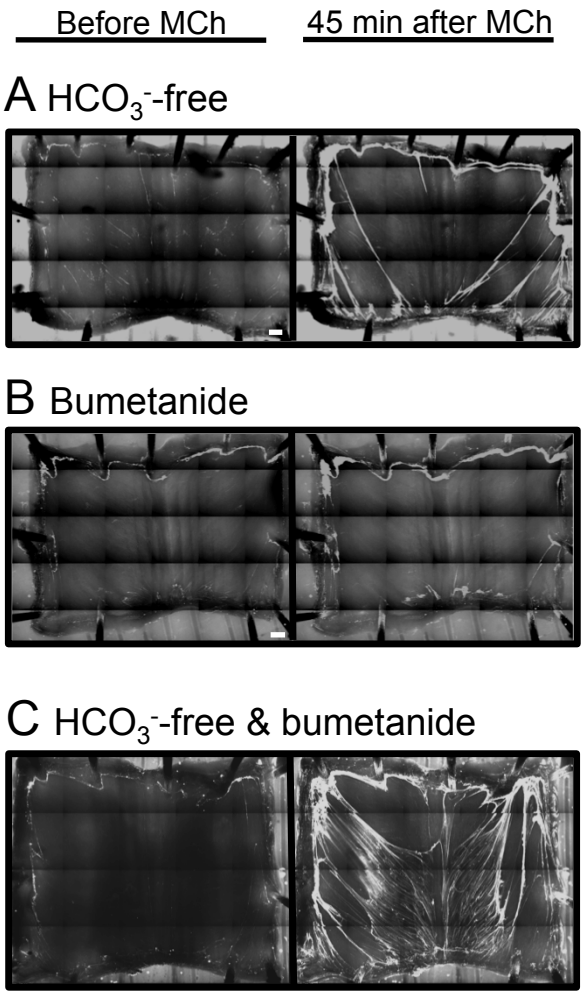
Before MCh
45 min after MCh
A HCO_3^--free
B Bumetanide
C HCO_3^--free & bumetanide